

Research Article

Control Allocation Design of Reaction Control System for Reusable Launch Vehicle

Rongjun Mu and Xin Zhang

School of Astronautics, Harbin Institute of Technology, Harbin 150001, China

Correspondence should be addressed to Rongjun Mu; [murjun@163.com](mailto:mu_rongjun@163.com)

Received 31 January 2014; Revised 13 April 2014; Accepted 13 April 2014; Published 12 June 2014

Academic Editor: Hui Zhang

Copyright © 2014 R. Mu and X. Zhang. This is an open access article distributed under the Creative Commons Attribution License, which permits unrestricted use, distribution, and reproduction in any medium, provided the original work is properly cited.

During the early stage of reusable launch vehicle (RLV) reentry flight, reaction control system (RCS) is the major attitude control device. RCS, which is much different from the atmospheric steer's control, requires a well designed control allocation system to fit the attitude control in high altitude. In this paper, an indexed control method was proposed for RCS preallocation, a 0-1 integer programming algorithm was designed for RCS allocation controller, and then this RCS scheme's effect was analyzed. Based on the specified flight mission simulation, the results show that the control system is satisfied. Moreover, several comparisons between the attitude control effect and RCS relevant parameters were studied.

1. Introduction

In the reentry flight phase, the aerodynamic characteristics of RLV vary rapidly, when serious uncertainties and nonlinearity exist. Therefore, RLV needs high robust and accurate attitude control algorithm. Different from normal vehicles, RLV usually relies on aerosurfaces and reaction control system for attitude control [1]. In its on-orbit operation and the initial reentry, RCS is the major attitude control device. Because the dynamic pressure is not strong enough for aerosurfaces to meet the needs of spacecraft attitude control.

Many control methods had already been presented to solve the attitude control problem of RLV with hypersonic speed. In [2], a variable structure control was used to control the attitude of RLV in ascent and reentry phases in case of small disturbance. In [3], a neural network algorithm was adopted to learn 7 level fuzzy rules online. This method has the problems of a large amount of computation and low reliability. Currently, the conventional gain-scheduling technique, called operating point-based linearization, can be applied for the nonlinear controller designing.

In this study, the attitude control algorithm is only designed for RCS [4–7]. The control moment from control law is handled by RCS command logic and operation logic to yield the final commands of thrusters [8]. Usually, RCS

consists of several thrusters. Naturally, the actual control moments [9] are produced by thruster ejecting the propellant from the jet. In consequence, the control allocation [10–14] between all the thrusters of RCS should be the key in the attitude control algorithm designing [15] (see Figure 1).

Therefore, the rest of the paper is organized as follows. The nonlinear model and control model of RLV are presented in Section 2. In Section 3, RCS is extensively studied and modeled. An indexed control method is proposed for RCS preallocation, and a 0-1 integer programming algorithm is designed for RCS control allocation in Section 4. Sections 5 and 6, respectively, give the RCS scheme's simulation results and the concluding remarks.

2. Mathematical Model of RLV

2.1. Nonlinear Model. In this study, a high-fidelity RLV model is used to demonstrate the proposed reliable control approach. The body configuration of RLV provides the inertial coupling in the lateral/directional channel. Hence, the dynamic model of RLV is a complicated and highly nonlinear time-variation uncertain system [16].

In modeling, the English-American coordinates system is used [17]. To simplify the complex model [18], some

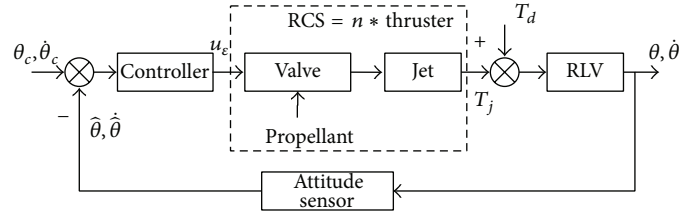


FIGURE 1: Block diagram of RCS.

installation errors, such as RCS thruster location error, are ignored and several assumptions are made as follows:

- take RLV as an ideal rigid body, and ignore any elastic vibration;
- its sideslip angle is small enough to make little angle assumption; thus, the lateral moments are provided mainly by RCS;
- the RLV principal axes of inertia and the body axes are superposed, regardless of the influence of inertia product;
- the dynamic characteristics of the navigation device are ignored, considering the vehicle's state can be obtained in time.

Then, the dynamic model of the reusable launch vehicle can be expressed as

$$\frac{dx}{dt} = v_x, \quad \frac{dy}{dt} = v_y, \quad \frac{dz}{dt} = v_z. \quad (1)$$

The attitude motion model of RLV is represented by

$$\begin{bmatrix} \dot{\phi} \\ \dot{\psi} \\ \dot{\gamma} \end{bmatrix} = \begin{bmatrix} \frac{1}{\cos \psi} (\omega_{y1} \sin \gamma + \omega_{z1} \cos \gamma) \\ \omega_{y1} \cos \gamma - \omega_{z1} \sin \gamma \\ \omega_{x1} + \tan \psi (\omega_{y1} \sin \gamma + \omega_{z1} \cos \gamma) \end{bmatrix} \quad (2)$$

$$(\psi \neq \pm 90^\circ).$$

During the initial reentry process, the translational equation of RLV can be described as

$$m\dot{V} = G + R + F_{co} + F_{rel} + F_k + F_w, \quad (3)$$

where G is referred to as gravity; R corresponds to the aerodynamic force; F_{co} is the control force, which is provided by RCS; F_{rel} and F_k are, respectively, convected force and Coriolis force, which are small enough to be neglected; the remaining F_w covers all the disturbing force.

The equations of rotation around the centroid can be described as

$$\begin{aligned} I_x \dot{\omega}_{x1} + (I_z - I_y) \omega_{y1} \omega_{z1} &= M_x, \\ I_y \dot{\omega}_{y1} + (I_x - I_z) \omega_{x1} \omega_{z1} &= M_y, \\ I_z \dot{\omega}_{z1} + (I_y - I_x) \omega_{x1} \omega_{y1} &= M_z, \end{aligned} \quad (4)$$

where the variables I_x, I_y, I_z are moments of inertia [19]; the variables M_x, M_y, M_z represent all the external moment around the body axis x, y, z of RLV.

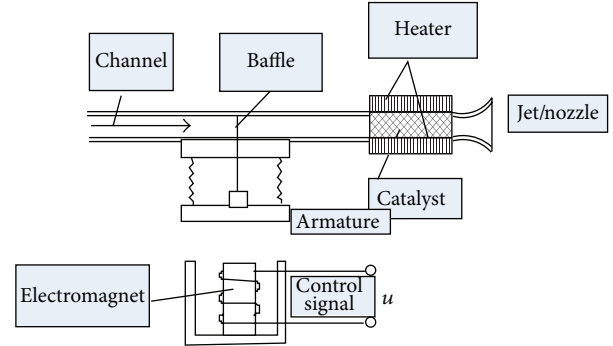


FIGURE 2: Thruster structure diagram.

2.2. Control Model. Respectively denote attack angle α , yaw angle ψ , roll angle γ , and the angular velocity of rotation $\omega_x, \omega_y, \omega_z$ as state variables of the control system. So we adopt the control model [20]:

$$\begin{aligned} \dot{\alpha} &= \omega_z - \frac{qs}{mV} (C_y^\alpha \alpha + C_y^{\delta_z} \delta_z), \\ \dot{\beta} &= \omega_x \sin \alpha + \omega_y \cos \alpha + \frac{qs}{mV} (C_z^\beta \beta + C_z^{\delta_y} \delta_y), \\ \dot{\gamma} &= \omega_x, \\ \dot{\omega}_x &= \frac{M_x}{I_x} + \frac{(I_y - I_z) \omega_y \omega_z}{I_x}, \\ \dot{\omega}_y &= \frac{M_y}{I_y} + \frac{(I_z - I_x) \omega_z \omega_x}{I_y}, \\ \dot{\omega}_z &= \frac{M_z}{I_z} + \frac{(I_x - I_y) \omega_x \omega_y}{I_z}. \end{aligned} \quad (5)$$

In this paper, during the RCS-only working stage, the control efficiency of the aerosurfaces is not strong enough compared with RCS. So the aerodynamic moment generated by the rudders can be ignored.

3. Mathematical Models for RCS

3.1. RCS Characteristics. Before illuminating the characteristics of the reaction control system, this paper needs to clarify its working process, which is simply outlined by Figure 2.

When the thruster does not work, the baffle, under the tension of the spring, blocks the propellant pipeline. So

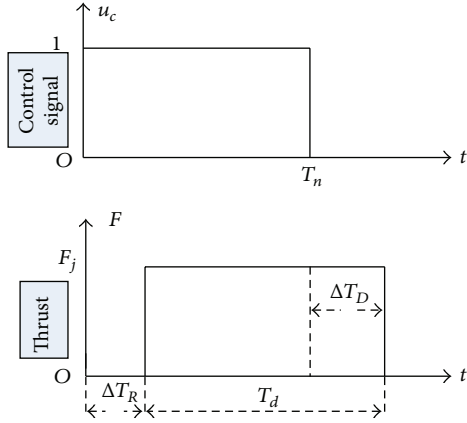


FIGURE 3: Thruster mathematical model.

the propellant cannot flow to the catalyst. Therefore there is no thrust. When a positive control signal is generated, the electromagnet will produce an attraction force to the armature. When the suction is larger than the tension of the spring, the armature will pull the baffle away. Then after the propellant meets the catalyst layer, chemical reaction will occur, which can generate heat and thrust. Conversely, when the suction is less than the spring force, armature will come back to the original position, and the reaction will be cut off.

By understanding the working process of RCS, the study concludes the following advantages [21]:

- (1) the thruster can work at any orbital position; thus RCS has already been widely used in spacecraft attitude control;
- (2) control moment, provided by RCS, along the RLV body axis is far greater than the coupling torque, which makes control logic more simple and flexible;
- (3) compared to the external and internal disturbance torques, RCS control moment is larger and has shorter transition time, so the disturbance torques can be neglected in the primary design stage of the control system;
- (4) RCS is applicable to nonperiodic disturbance torque occasions. Due to the consumption of propellant, its service life is short, which makes it suitable for Space Shuttle, RLV, and recoverable satellite;
- (5) thrusters usually adopt the stationary force [22, 23] and the ON/OFF switch working mode.

Certainly, RCS has several following disadvantages [24]:

- (1) RCS needs propellant to produce control moment, but the propellant is limited;
- (2) lateral jet has the complex aerodynamic interference to the rudders, especially in the phase of hypersonic speed;
- (3) it is difficult to maintain the continuous and uniform jet flux, which results in more difficulty for the control scheme designing;

- (4) as one thruster can only produce one direction of force and moment, the control system may require more than one of them to produce various directions of attitude control moment. Usually 6 thrusters can complete the attitude control task [25]. But considering the reliability, the actual system always needs the necessary redundancy. For example, the RCS in this paper has 12 thrusters.

3.2. *Thruster Model.* Considering electromagnetic hysteresis and nonlinear characteristics of the thruster, the relationship between the control signal and the thrust output is complicated and nonlinear. Therefore, according to specific requirements, some practical mathematical models [26] for the thruster are given as follows.

(1) *Ideal Mathematic Model.* This model is relatively simple, without considering the thrusters' ON/OFF switching delay, and assuming that the thrust output is constant.

This ideal thruster model is usually used for the theory validation, preliminary design, and mathematical analysis.

(2) *Mathematical Model Considering Switching Delay.* This model is more accurate than the ideal one. It considers the thrusters' ON/OFF switching delay, but still ignores the nonlinear dynamic characteristics during the ON/OFF switching process. Figure 3 gives the curve of thrust output versus time.

Usually, this model is used at the design and analysis stage of attitude control system.

(3) *The Index Mathematical Model.* This model considers both the time delay and the dynamic characteristics during the ON/OFF switching (the thrust rises or falls like the exponential function). So, obviously this model, usually used at the simulation stage, is the most precise among the three.

Taking account of time delay and the dynamic characteristics during the switching process, the thruster model is built by using Matlab/Simulink (Figure 4).

In Figure 4, the module of "Transport Delay" represents the switching time delay of the thruster; the variable "delta1" in the module of "Transfer Fcn" represents the switching on acceleration; the variable "delta2" in the module of "Transfer Fcn1" represents the switching off deceleration. Figure 5 gives the simulation curve of thruster model responding to the control command signal.

3.3. *Force and Moment of RCS.* Figures 6 and 7 present the thrusters layout map, which shows the jet directions and positions of the 12 thrusters.

The output of the i th thruster is

$$F_{R_i} = \begin{bmatrix} 0 \\ F_i \cos \varepsilon_i \\ F_i \sin \varepsilon_i \end{bmatrix} \quad M_{R_i} = F_{R_i} \times \begin{bmatrix} x_i - x_c \\ y_i - y_c \\ z_i - z_c \end{bmatrix}, \quad (6)$$

where F_i is the resultant force of thruster i ; ε_i is the deflection angle of corresponding jet; control moment M_{R_i} is the cross product of F_{R_i} and its corresponding force arm relative to the center of mass.

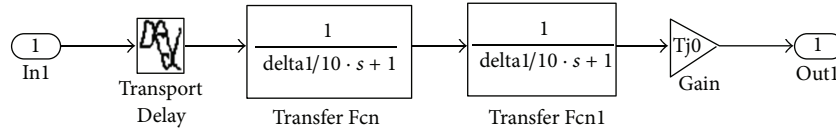


FIGURE 4: The thruster model in Simulink.

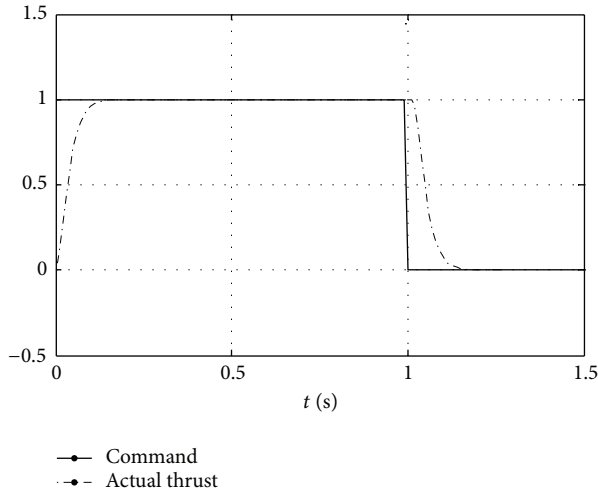


FIGURE 5: The response curve of thruster model to control command.

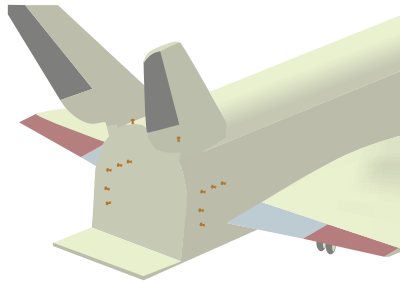


FIGURE 6: Thrusters longitudinal layout map.

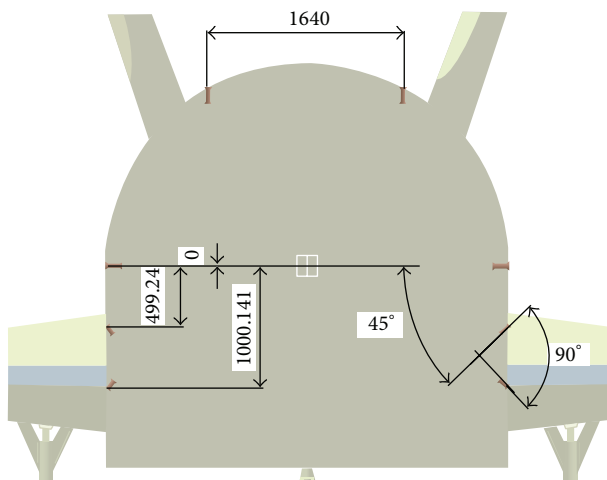


FIGURE 7: Thrusters lateral layout map.

TABLE 1: Control moments of thrusters.

No.	Roll moment (kN*m)	Yaw moment (kN*m)	Pitch moment (kN*m)
1	-0.82	0	+14.22
2	+0.82	0	+14.22
3	+0.17	+14.22	0
4	-0.17	-14.22	0
5	+0.17	+13.77	0
6	-0.17	-13.77	0
7	+0.17	+13.31	0
8	-0.17	-13.31	0
9	-1.42	+10.06	+10.06
10	+1.42	-10.06	+10.06
11	+0.59	+10.06	-10.06
12	-0.59	-10.06	-10.06

Based on (6), the control moments of all the thrusters can be obtained in Table 1.

According to Table 1, a thruster alone can produce at least two axes control moment, which makes specific control unsuccessful; with the proper selection of thrusters, we can achieve a variety of control moment levels to ensure the hardware redundancy of RCS.

4. Design of Control Allocation

The designed control allocation system consists of two parts: preallocation unit and allocation controller unit. According to the configuration of RCS, the preallocation unit uses the indexed control method to select all the reasonable sets of thrusters and process the moment data of the entire thruster selection. For the allocation controller unit, the paper applies the 0-1 integer programming algorithm to select the optimal selection of thrusters to meet the expected control demands. By changing some parameters of the algorithm, this unit can ensure that the system achieves the optimal effect of the fuel consumption, control precision, and so on.

Figure 8 gives the block diagram of the RCS control allocation system. In the figure, the expected control moment, obtained by the gain-scheduling controller, is the input of the allocation system. Hence, considering the expected control demands and the entire available selections of thrusters given by the preallocation unit, the allocation controller can obtain the optimal selection and give the corresponding igniting command to the current actuator, namely, RCS. To the best of the authors' knowledge, this control allocation system can ensure RCS work normally even with some thrusters failure.

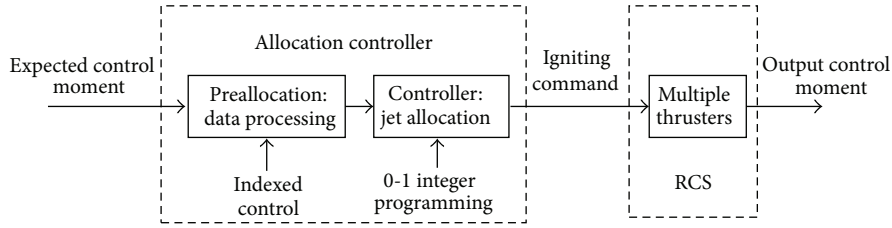


FIGURE 8: RCS control allocation system diagram.

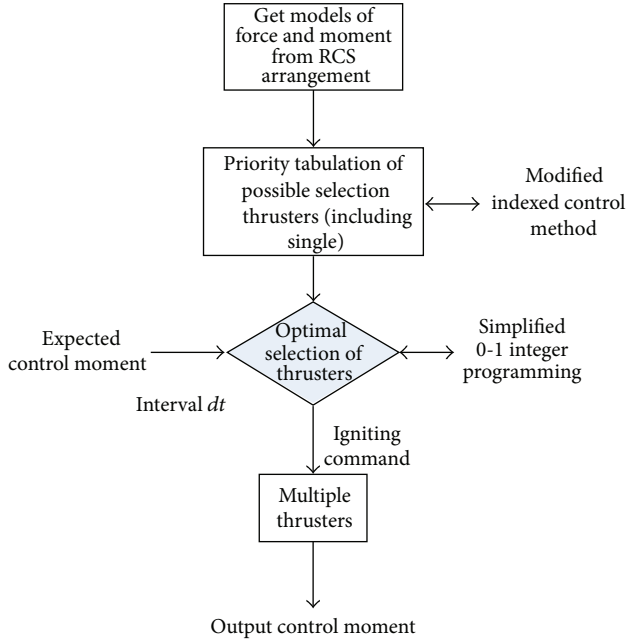


FIGURE 9: RCS control allocation flow diagram.

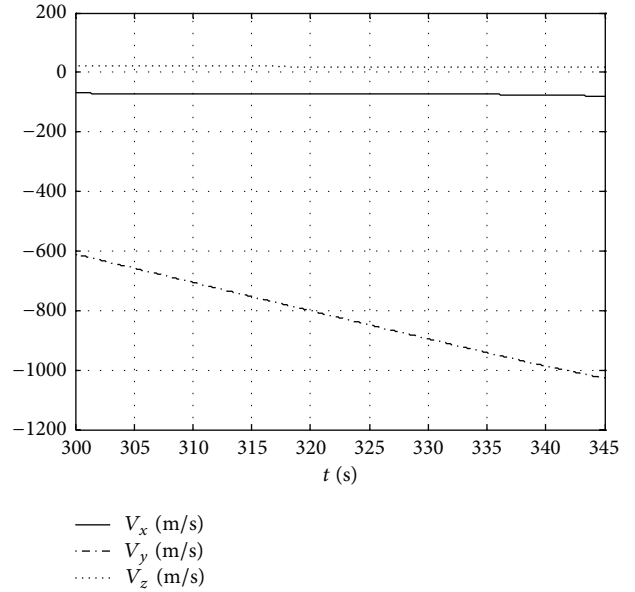


FIGURE 11: Simulation result of flight speed.

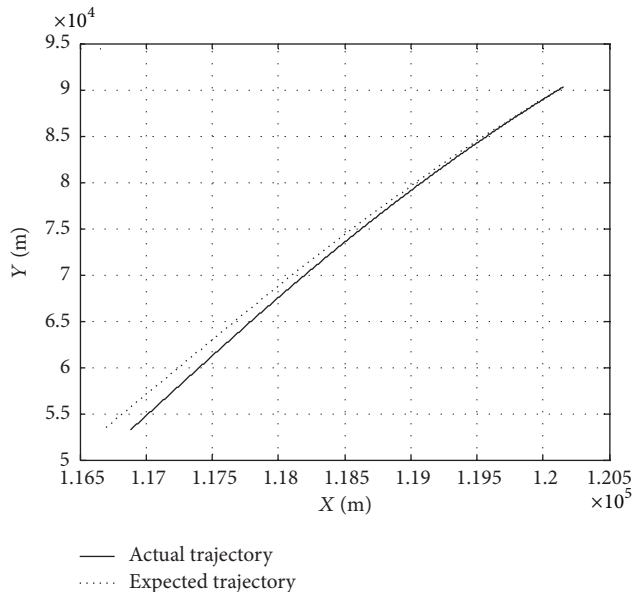


FIGURE 10: Simulation result of trajectory in 2D.

As we can see, the designed control allocation system has a lot of differences with the rudder control system. Also the control model of RLV needs some appropriate deduction and simplification. Generally, we need to consider the time delay characteristics, the dynamic characteristics of thrusters' ON/OFF switching, the minimum pulse limit (define the variable dt as the minimum interval of two thruster selections, i.e., the shortest interval between the ignition and shutdown of each thruster), the maximum ignition duration, the total ON/OFF switching times, and the fuel consumption [27].

4.1. RCS Preallocation Method. According to Figure 8, the first task of preallocation is to decide how to get all the reasonable sets of thrusters. When choosing the RCS thruster selection, we should follow the following principles [28]:

- (1) during the thruster selection, try not to bring additional coupling moment;
- (2) choose the selection with the larger control moment arm, since it is good to reduce the consumption of RCS;

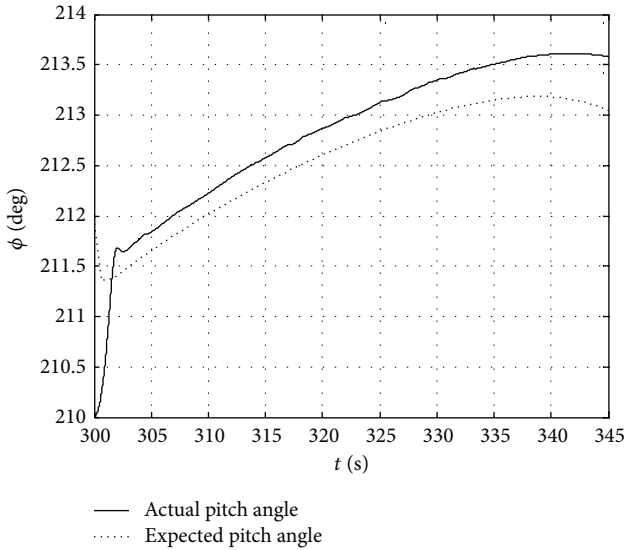


FIGURE 12: Simulation result of pitch angle.

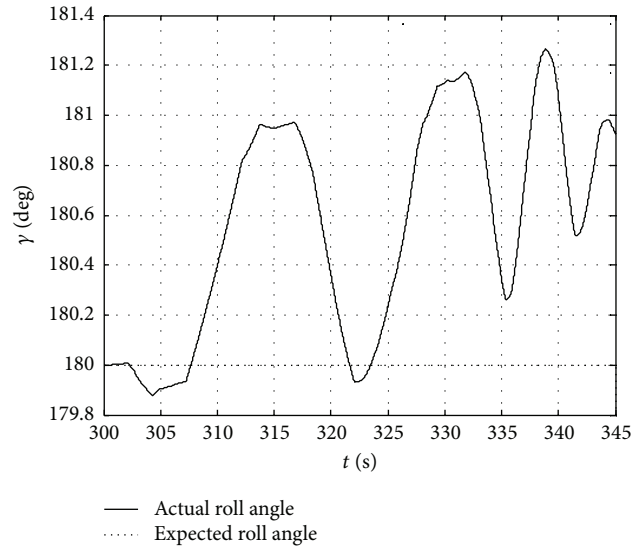


FIGURE 14: Simulation result of roll angle.

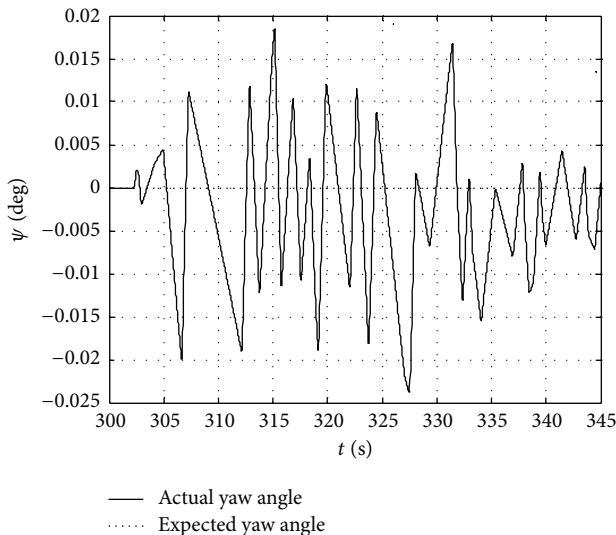


FIGURE 13: Simulation result of yaw angle.

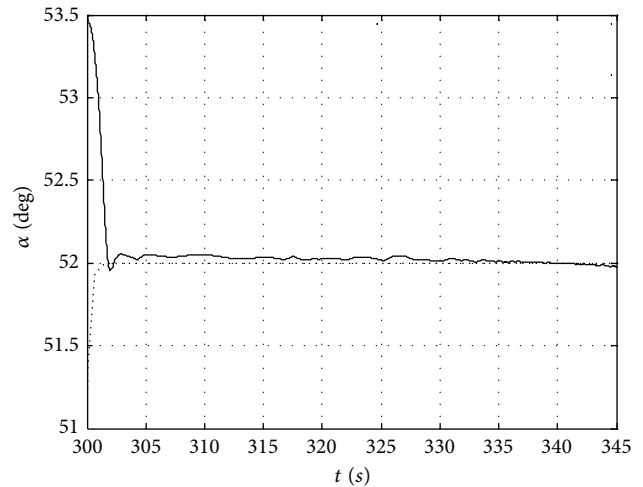


FIGURE 15: Simulation result of attack angle.

- (3) in order to improve the redundancy of the system, normally choose the selection with the higher priority.

Based on the above principles, we can get all the possible and reasonable thruster selections, which is essential for the next data process.

This preallocation unit is to process data, where all the preparation for the control allocation is accomplished. In [24], there are three methods for data processing: dependent control method, graded control method, and indexed control method.

(1) *The Dependent Control Method.* According to this method, the resultant moment of each selection is parallel with one of the body axes, so that there is no coupling problem. And if

a thruster is in this selection, it cannot be in any other selection. Although this method does not fully utilize all the thrusters, it is logically simple and really simplifies the process. However, when one thruster fails, RCS may lose the control ability, which means the system's redundancy is zero.

(2) *The Graded Control Method.* This method is an improvement on the first one in terms of the thruster utilization. The difference between the two methods is whether a thruster can be used in more than one selection. Therefore, in a way, this method relatively increases the redundancy of the system.

(3) *The Indexed Control Method.* This method takes all the possible selections of thrusters (considering the single thruster situation) into consideration and ranks them by

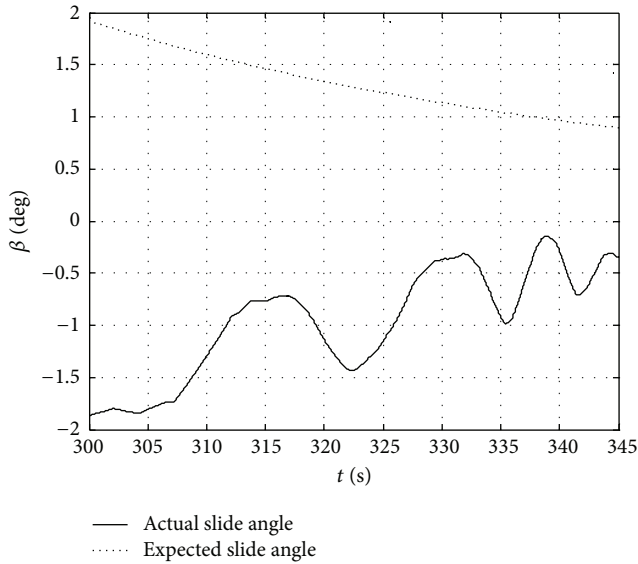


FIGURE 16: Simulation result of slide angle.

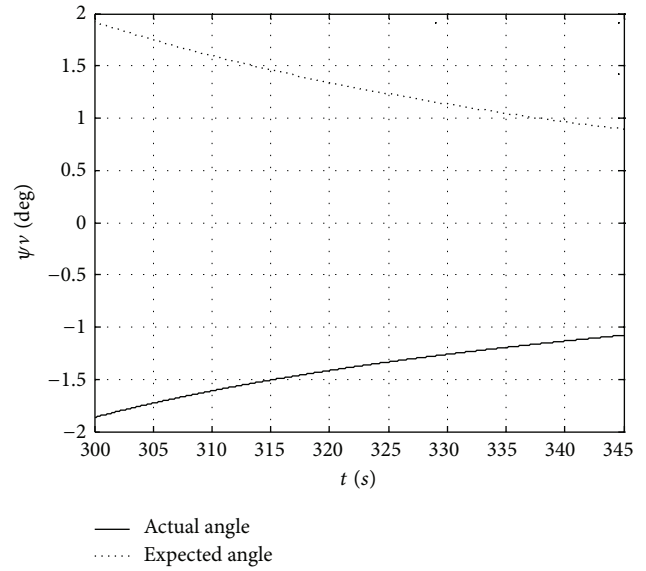


FIGURE 18: Simulation result of trajectory deflection angle.

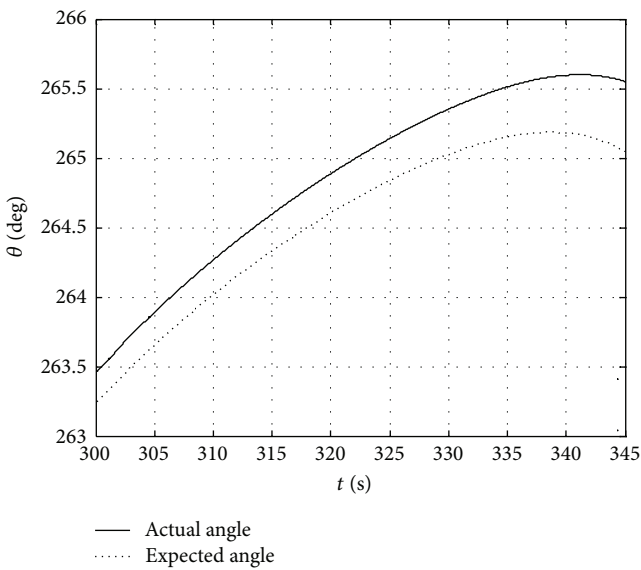


FIGURE 17: Simulation result of flight path angle.

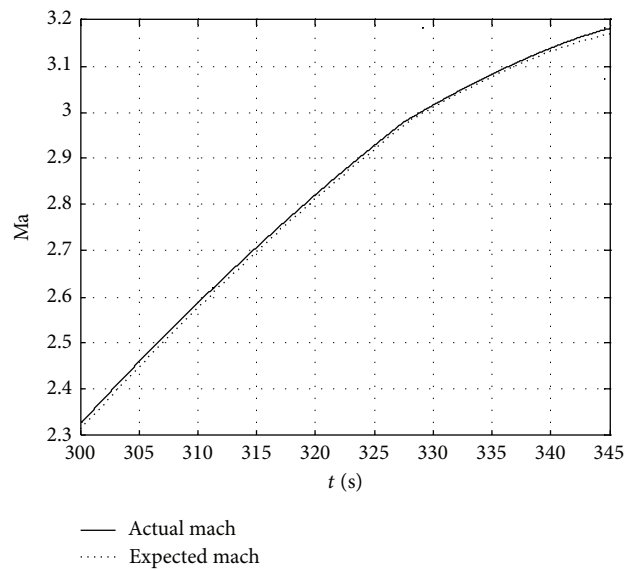


FIGURE 19: Simulation result of Mach number.

using the expected control moment as the index or criteria for evaluation. So if the moment of the selection is closer to the expected moment, its priority is higher.

The indexed control method has the largest redundancy among the three methods and guarantees that the system works normally even when some thrusters fail. However, compared to the other two methods, this one needs to establish large tables of data, covering all reasonable and available thruster selection. But after modifying the method by adding the selection principals into the method as a filter, the amount of calculation can be reduced greatly.

In this paper, RCS can have only 12 thrusters, and some of them have serious coupling moment between pitching

and rolling channels. Therefore, the modified indexed control method is the best solution.

4.2. RCS Control Allocation Method. Denote

$$\Delta M = |M_C - M|, \tag{7}$$

where the variable M_C is the expected control moment, which is obtained by the gain-scheduling controller; the variable M is the actual control moment provided by RCS. As we all know, the closer the resultant control moment of the selection is to the expected moment, the better the selection is. That is to say, the less ΔM is, the better the selection is. Nevertheless, when the values of ΔM in two different selections are close to each other, the variables, such as the fuel consumption

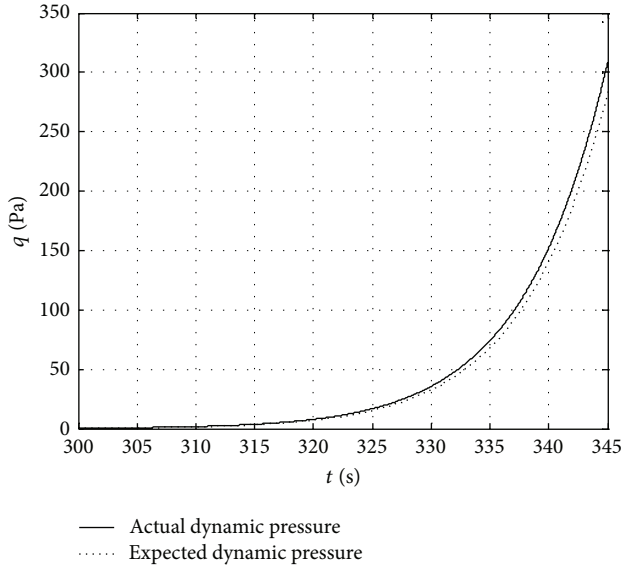


FIGURE 20: Simulation result of dynamic pressure.

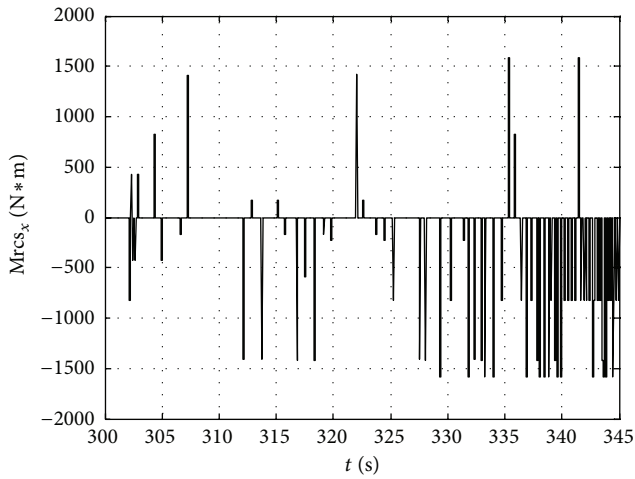


FIGURE 21: Simulation result of RCS roll moment.

and the number of selected thrusters, should be taken into account.

Thus, define the target function J_{RCS} as [29, 30]

$$\begin{aligned} \min J_{\text{RCS}} &= \{w_{\text{th}}u_M + w_M |M_C - M|\} \\ \text{s.t. } M &= \sum_{i=1}^n M_i u_{M_i} \\ M &> M_C, \end{aligned} \quad (8)$$

where the variable n is the total number of the thrusters. Taking the RCS in this paper as an example, $n = 12$. The variable w_M is the priority of the corresponding selection. Or it can be regarded as the weight of this selection. Based on (8), the bigger the variable is, the worse the selection is.

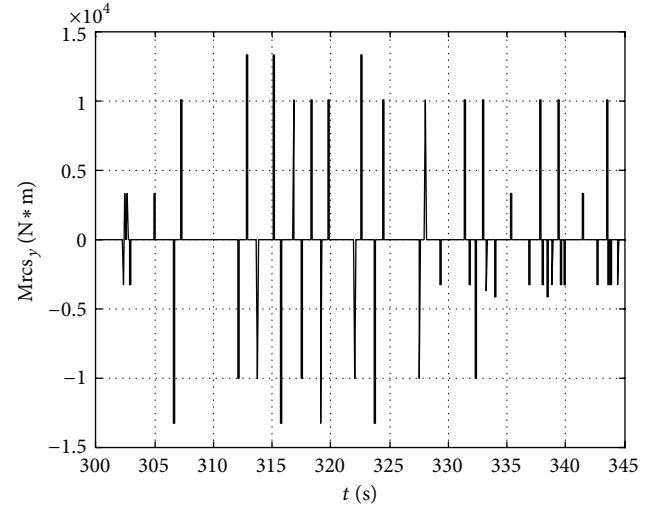


FIGURE 22: Simulation result of RCS yaw moment.

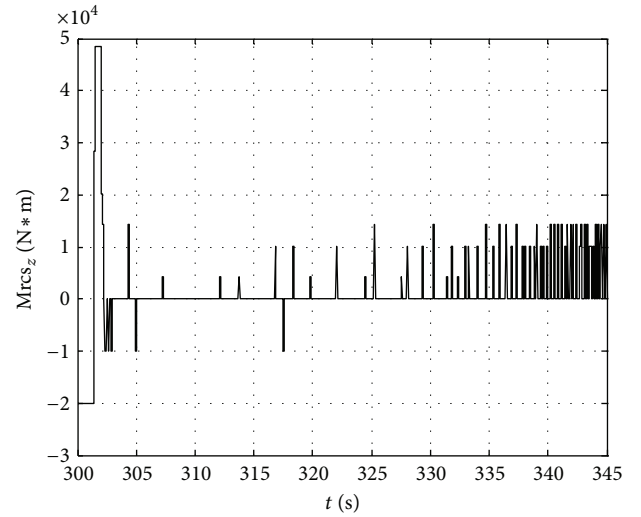


FIGURE 23: Simulation result of RCS pitch moment.

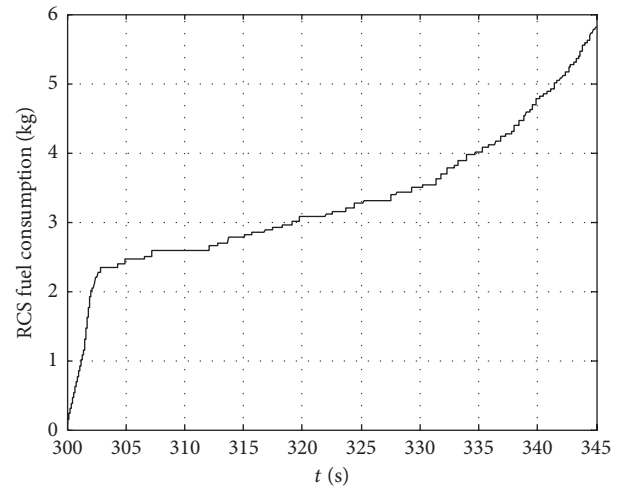


FIGURE 24: Simulation result of RCS consumption.

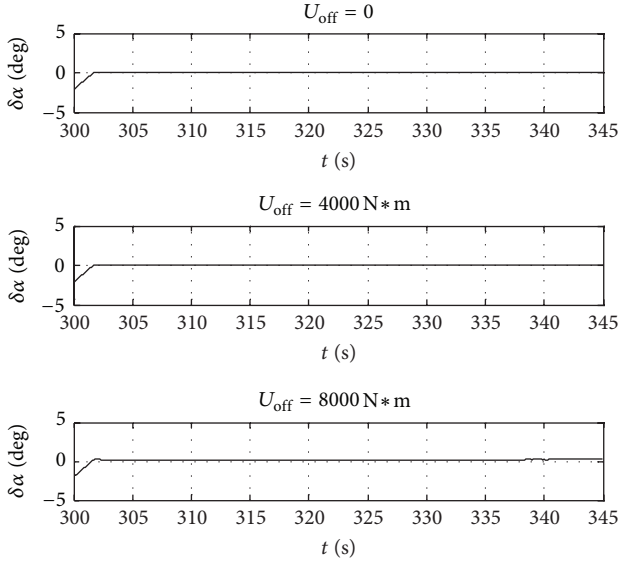


FIGURE 25: Simulation result of attack angle deviation.

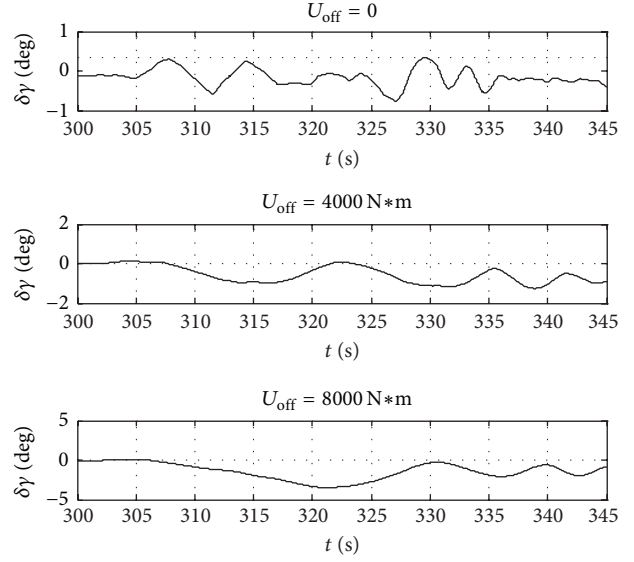


FIGURE 27: Simulation result of roll angle deviation.

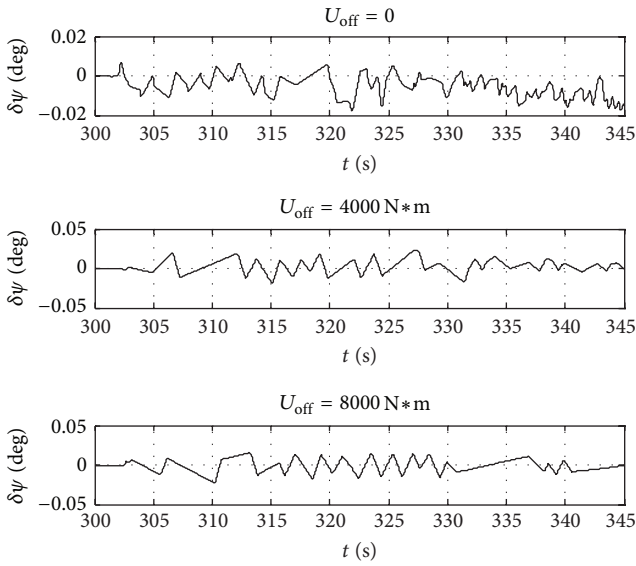


FIGURE 26: Simulation result of yaw angle deviation.

Define the vector w_{th} as

$$w_{th} = [w_{M_1}, w_{M_2}, \dots, w_{M_n}], \quad (9)$$

where the variable w_{M_i} ($i = 1, 2, \dots, n$) is the weight or the priority of the thruster i in this current selection. The bigger w_{M_i} is, the lower the priority is. The remaining variable u_M is the working condition of thruster i . For example, if only the 9th and 10th thrusters work, $u_M = [0 \ 0 \ 0 \ 0 \ 0 \ 0 \ 0 \ 0 \ 1 \ 1 \ 0 \ 0]^T$. In general terms, the closer the real moment is to the expected moment, the smaller the value of the target function is. The smaller the number of the selected thrusters is, the better the selection is.

Meanwhile, to reduce the consumption of propellant, define the range of the dead zone as $[-U_{off}, U_{off}]$ [31]. In this

range, the deviation of the attitude angles is too small to start the RCS thruster. So the larger U_{off} is, the lower the control precision is.

So, the control allocation problem can be described as the following 0-1 integer linear programming problem:

$$\begin{aligned} \min_{u_M, \Delta M} & [w_1 \ w_2 \ \dots \ w_n \ | \ w_M] \begin{bmatrix} u_M \\ \Delta M \end{bmatrix}, \quad \forall M_C \geq U_{off} \\ \text{s.t.} & \sum_{i=1}^n |M_i u_{M_i}| > M_C. \end{aligned} \quad (10)$$

According to (10), how to choose the values of the weight is the key of success or failure for this allocation method, as these values vary in different situations. So by the simplification of the weight, the programming model is modified to the following one:

$$\begin{aligned} \min J_0 & = \{u_M^T \cdot L_{12 \times l} + k \cdot U_{off} - M_C\} \\ \text{s.t.} & k = \text{sum}(u_M) \\ & 12 \leq l \leq \sum_{i=1}^{12} C_{12}^i, \end{aligned} \quad (11)$$

where the variable L is a 12-by- l matrix including the resultant force and moment of all the selections given by the preallocation unit; the variable l is the sum of all the reasonable and available selections; the variable k represents the sum of selected thrusters.

Based on the above analysis, the control allocation system is built by considering the current thruster configuration, the priority of selection, the deadweight of RCS, and so on. The designing process is described in Figure 9.

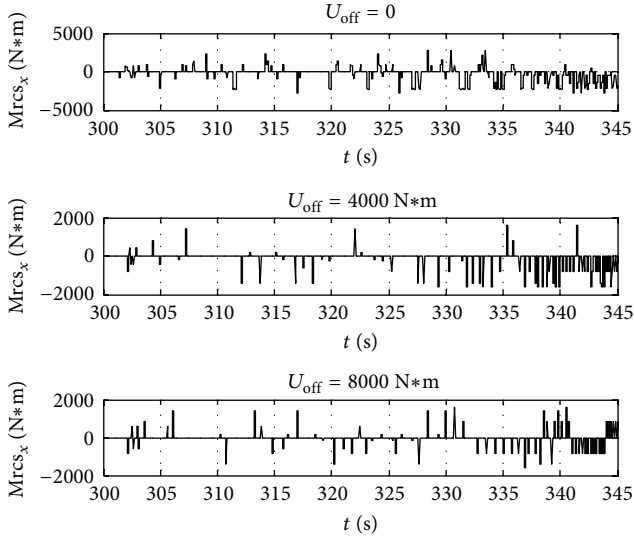


FIGURE 28: Simulation result of roll moment.

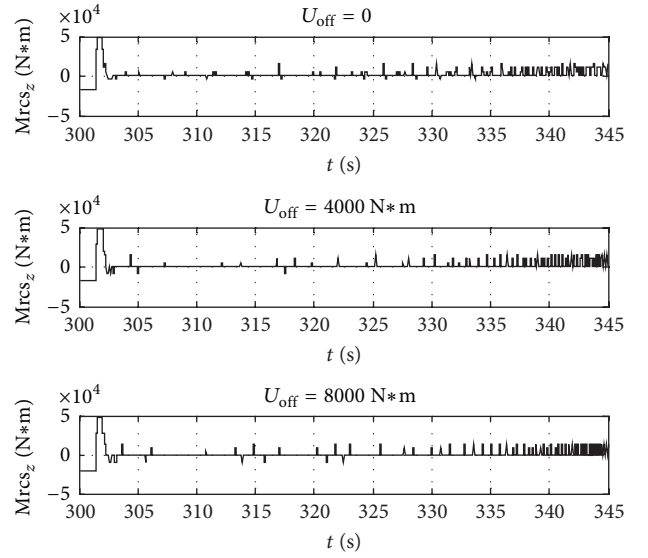


FIGURE 30: Simulation result of RCS pitch moment.

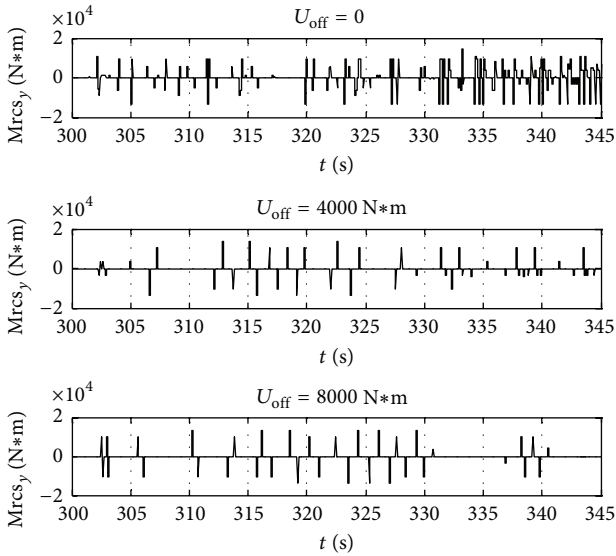


FIGURE 29: Simulation result of RCS yaw moment.

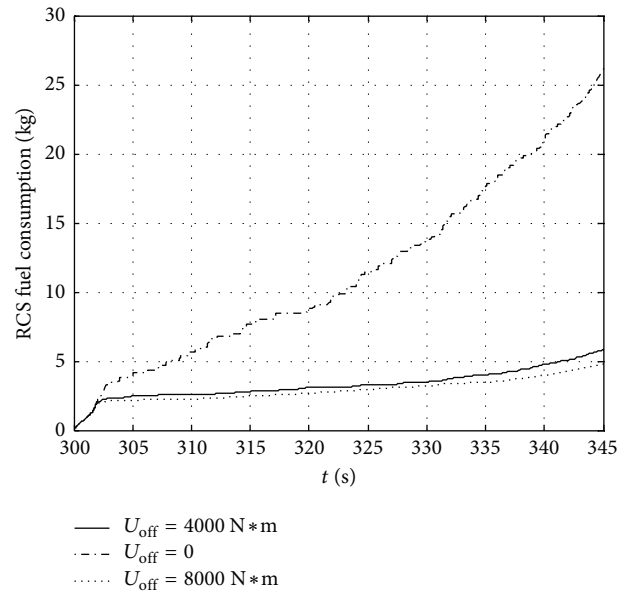


FIGURE 31: Simulation result of RCS consumption.

5. Mathematical Simulation

In the initial stage of reentry, reusable launch vehicle maintains the large attack angle (the boundary dynamic pressure is 300 Pa between RCS control stage and RCS/rudders [32, 33] compound control stage) [34]. At this time, the aerodynamic efficiency of the rudders is far not enough to meet the attitude control need. So the RCS control is the only way to achieve large angle attitude maintaining. Here by the mathematical simulation, we verify the control allocation strategies of RCS and make the comparison between the attitude control performance and RCS relevant parameters [35].

Initial conditions are as follows [36]:

$$\begin{bmatrix} x \\ y \\ z \end{bmatrix} = \begin{bmatrix} 102150 \\ 90308 \\ 4025 \end{bmatrix} \text{ m}$$

$$V = \begin{bmatrix} -71.8 \\ -605.4 \\ 20.5 \end{bmatrix} \text{ m/s} \quad (12)$$

$$\begin{bmatrix} \varphi \\ \psi \\ \gamma \end{bmatrix} = \begin{bmatrix} 212^\circ \\ 0^\circ \\ 180^\circ \end{bmatrix}.$$

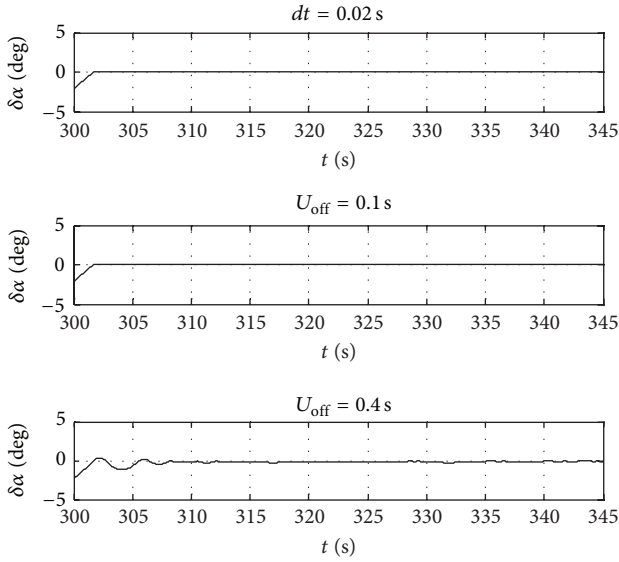


FIGURE 32: Simulation result of attack angle deviation.

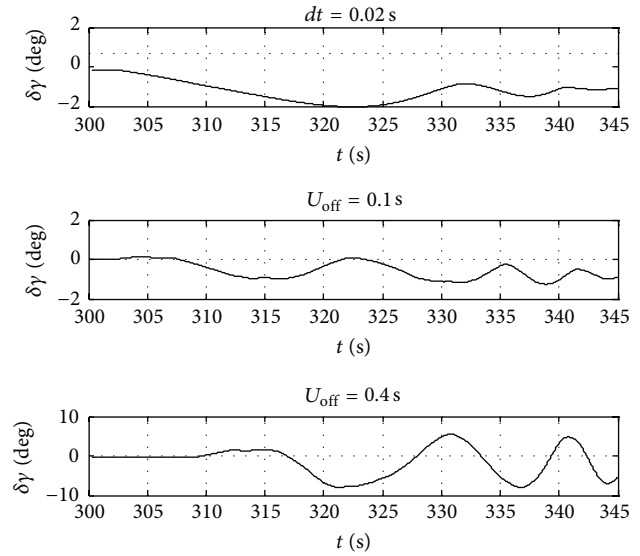


FIGURE 34: Simulation result of roll angle deviation.

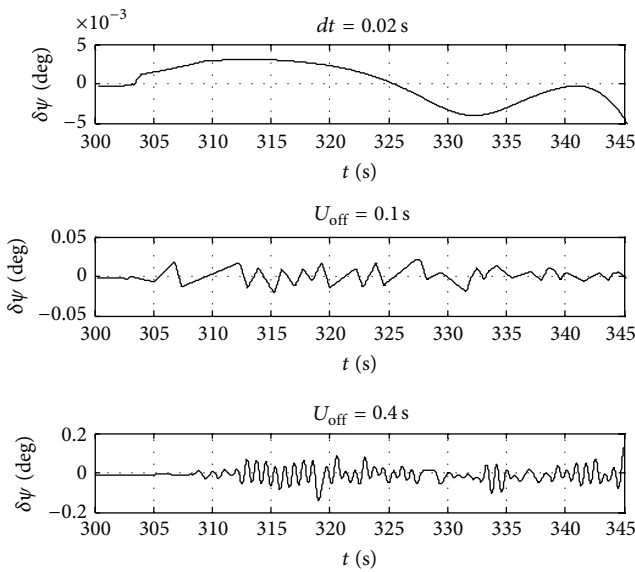


FIGURE 33: Simulation result of yaw angle deviation.

Simulation results of the RLV results are listed as follows.

(1) Weight $U_{off} = 4000 \text{ N} \cdot \text{m}$, the Selection Interval $dt = 0.1 \text{ s}$. Based on Figures 10, 11, 12, 16, 17, 18, 19, 20, 21, 22, 23, and 24, we find that the control precision declines as time goes on, and the consumption rate of RCS fuel at 340 s is far greater than ever. The reason is that along with the increase of the dynamic pressure, pneumatic restoring torque also increases, which decreases the efficiency of RCS control. Therefore, at the end of the simulation, only using RCS for attitude control becomes more and more difficult.

In the 0-1 integer programming algorithm, the allocations of pitch, yaw, and roll moments are interactional. So, considering that the expected rolling moment is relatively smaller

than the others, it has less effect on the control allocation. This will cause the rolling angle deviation to be the biggest in the three channels, as we can see by comparing Figures 13 and 14 with Figure 15. This characteristic is decided by the algorithm. It does not mean the controller of the roll channel failed.

(2) Comparisons between Different Selection Weights U_{off} . In order to analyze the influence of the different weights U_{off} on the allocation method and the control precision of RCS, respectively, set U_{off} as 0, 4000 $\text{N} \cdot \text{m}$, and 8000 $\text{N} \cdot \text{m}$, and keep the selection interval dt as 0.1 second. The simulation results are shown in Figures 28, 29, and 30.

By the comparisons between different selection weights U_{off} , we conclude that the fuel consumption of RCS will be reduced to a certain extent when the U_{off} increase. In Figure 31, the consumption of $U_{off} = 4000 \text{ (N} \cdot \text{m)}$ is much less than that of $U_{off} = 0$, but the consumption of $U_{off} = 8000 \text{ (N} \cdot \text{m)}$ is approximates to that of $U_{off} = 4000 \text{ (N} \cdot \text{m)}$.

Also, based on Figures 25, 26, and 27, the increase of U_{off} will decrease the control precision, especially for the yaw and roll channels. The reason is that the selection result of the RCS allocation method is mainly influenced by the biggest expected moment demand. In this case, the expected control moment of the pitch channel is much bigger than the others. So the pitch angle control precision is the highest and rolling angle control accuracy is the worst.

(3) Comparisons between Different Thruster Selection Intervals dt . In order to analyze the influence of the different thruster selection intervals dt on the allocation method and the control precision of RCS, respectively, set dt as 0.02 second, 0.1 second, and 0.4 second, and keep weight U_{off} as 4000 $\text{N} \cdot \text{m}$. The simulation results are shown in Figures 32, 33, 34, and 38.

From the simulation comparisons of different intervals, we learn that the shorter the single selection interval is the higher the control precision is. But at the same time,

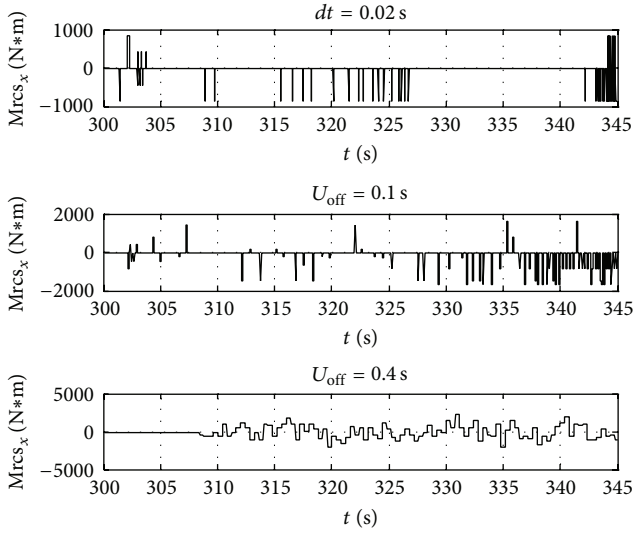


FIGURE 35: Simulation result of RCS roll moment.

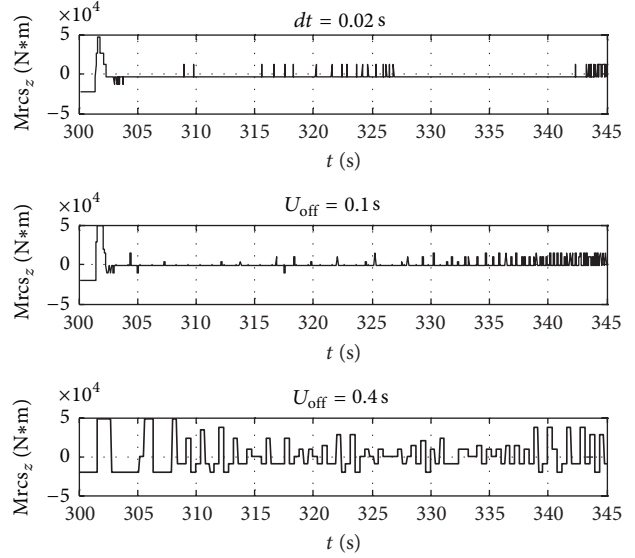


FIGURE 37: Simulation result of RCS pitch moment.

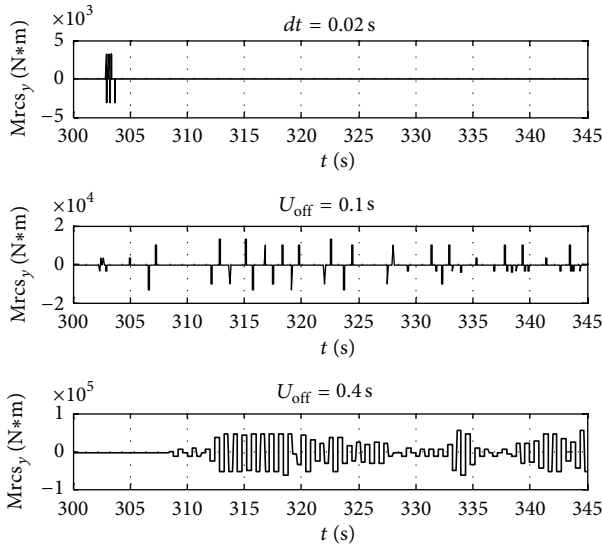


FIGURE 36: Simulation result of RCS yaw moment.

according to Figures 35, 36, and 37, we can see that the frequency of thruster's switching ON/OFF has greatly increased, which will reduce the service life of RCS. Hence, the interval should be properly decided according to actual demand.

6. Conclusion

This paper designs the control allocation method of reaction control system for reusable launch vehicle. A modified indexed control method has been presented to solve the data processing at the preallocation stage, and a simplified 0-1 integer programming algorithm has been proposed to design the allocation controller. To demonstrate the scheme, a series of mathematical simulations in different control allocation strategies of RCS has been made. The results

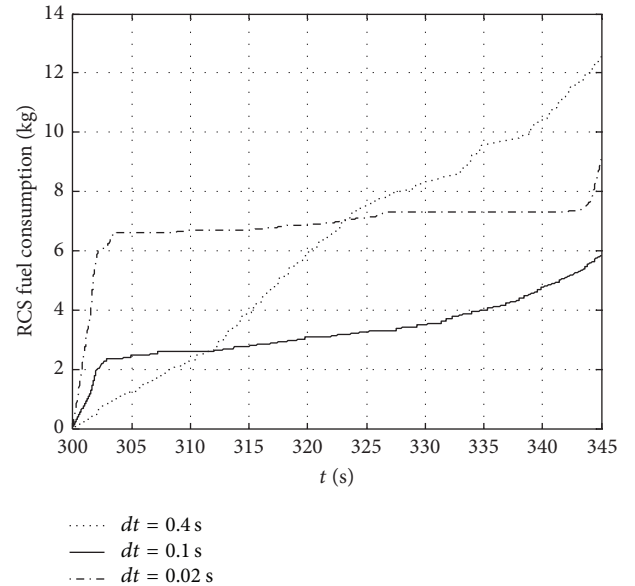


FIGURE 38: Simulation result of RCS consumption.

show that the designed RCS control allocation method can effectively handle tracking accuracy and robustness in the initial reentry phase. Moreover, the method proposed in this paper can readily be applied to the design of reliable allocation controllers.

Conflict of Interests

The authors declare that there is no conflict of interests regarding the publication of this paper.

References

- [1] Z. Jun, J. Pengfei, and H. Weijun, "Attitude control algorithm for reusable launch vehicle in reentry flight phase," *Journal of China Ordnance*, vol. 5, no. 1, pp. 15–19, 2009.
- [2] Y. Shtessel and J. McDuffie, "Sliding mode control of the X-33 vehicle in launch and re-entry modes," in *Proceedings of the Guidance, Navigation and Control Conference and Exhibit*, pp. 1352–1362, AIAA, Boston, Mass, USA, 1998.
- [3] Y. Fengxian, L. Hua, and Z. Li-Jun, "The application of the fuzzy-neural network controller of the flighter pose control," *Aerospace Control*, vol. 17, no. 1, pp. 43–49, 1999 (Chinese).
- [4] C. A. Tobin, W. Bong, and C. Stanley, "Pulse-modulated control synthesis for a flexible spacecraft," *Journal of Guidance Control, and Dynamics*, vol. 13, no. 6, pp. 1014–1022, 1990.
- [5] M. Piero and C. LePome Robert, "Design of a model predictive control flight control system for a reusable launch vehicle," in *Proceedings of the Guidance, Navigation and Control Conference and Exhibit*, pp. 5360–5370, AIAA, Austin, Tex, USA, 2003.
- [6] D. S. Rubenstein and D. W. Carter, "Attitude control system design for return of the kistler KI orbital vehicle," *AIAA*, vol. 4420, pp. 1410–1422, 1998.
- [7] T. Ieko, Y. Ochi, and K. Kanai, "New design method for pulse-width modulation control systems via digital redesign," *Journal of Guidance, Control, and Dynamics*, vol. 22, no. 1, pp. 123–128, 1999.
- [8] Z. Jun, J. Pengfei, and H. Weijun, "Design of neural network variable structure reentry control system for reusable launch vehicle," *Journal of China Ordnance*, vol. 4, no. 3, pp. 191–197, 2008.
- [9] N. Guodong, "Research on reaction control system for spacecraft re-entry flight," *Flight Dynamics*, vol. 23, no. 3, pp. 16–19, 2005 (Chinese).
- [10] T. Ting and N. Flanagan, "Space shuttle transition controller OMS-TVC and RCS jet thruster stability analysis," Tech. Rep. AIAA-91-2220, 1991.
- [11] V. E. Haloulakos, "Thrust and impulse requirements for jet attitude-control systems," Tech. Rep. AIAA-63-237, 1963.
- [12] J. D. Gamble, K. M. Spratlin, and L. M. Skalecki, "Lateral directional requirements for a low L/D aero-maneuvering orbital transfer vehicle," Tech. Rep. AIAA-84-2123, 1984.
- [13] R. Taylor, "Adaptive attitude control for long-life space vehicles," Tech. Rep. AIAA-69-945, 1969.
- [14] F. Bernelli-Zazzerà and P. Mantegazza, "Pulse-width equivalent topulse-amplitude discrete control of linear systems," *Journal of Guidance, Control, and Dynamics*, vol. 15, no. 2, pp. 461–467, 1992.
- [15] A. S. Hodel and R. Callahan, "Autonomous Reconfigurable Control Allocation (ARCA) for reusable launch vehicles," Tech. Rep. 2002-4777, AIAA, 2002.
- [16] F. Liao, J. L. Wang, E. K. Poh, and D. Li, "Fault-tolerant robust automatic landing control design," *Journal of Guidance, Control, and Dynamics*, vol. 28, no. 5, pp. 854–871, 2005.
- [17] W. Sentang and F. Yuhua, *Flight Control System*, Beijing University of Aeronautics and Astronautics Press, 2006 (Chinese).
- [18] P. P. Khargonekar, K. Poolla, and A. Tannenbaum, "Robust control of linear time-invariant plants using periodic compensation," *IEEE Transactions on Automatic Control*, vol. 30, no. 11, pp. 1088–1096, 1985.
- [19] B. N. Pamadi and G. J. Brauckmann, "Aerodynamic characteristics, database development and flight simulation of the X234 vehicle," in *Proceedings of the 38th Aerospace Sciences Meeting and Exhibit*, pp. 900–910, AIAA, Reno, Nev, USA, 2000.
- [20] W. R. Van Soest, Q. P. Chu, and J. A. Mulder, "Combined feedback linearization and constrained model predictive control for entry flight," *Journal of Guidance, Control, and Dynamics*, vol. 29, no. 2, pp. 427–434, 2006.
- [21] W. Wenzheng, *Research on Composite Control Using Aero Control Surface and RCS*, China Aero Dynamic Research and Develop Center, Mianyang, China, 2005 (Chinese).
- [22] D. Zimpfer, "On-orbit flight control design for the Kistler K-1 reusable launch vehicle [R]," AIAA Paper 99-4210, 1999.
- [23] C. Zimmerman and G. Duckeman, "An automated method to compute orbital re-entry trajectories with heating constraints," AIAA Paper A0237761, 2002.
- [24] Y. Fang, "Reaction control system control method for reusable launch vehicle," *Acta Aeronautica et Astronautica Sinica*, vol. 29, pp. 97–101, 2008 (Chinese).
- [25] P. A. Servidia and R. S. Sánchez Peña, "Thruster design for position/attitude control of spacecraft," *IEEE Transactions on Aerospace and Electronic Systems*, vol. 38, no. 4, pp. 1172–1180, 2002.
- [26] C. S. Qian, Q. X. Wu, C. S. Jiang, and L. Zhou, "Flight control for an aerospace vehicle's reentry attitude based on thrust of reaction jets," *Journal of Aerospace Power*, vol. 23, no. 8, pp. 1546–1552, 2008 (Chinese).
- [27] H. Chenglong, C. Xin, and W. Liaoni, "Research on attitude control of reaction control system for reusable launch vehicle," *Journal of Projectiles, Rockets, Missiles and Guidance*, vol. 30, no. 1, pp. 51–57, 2010 (Chinese).
- [28] H. Weijun and Z. Jun, "Research on revised pulse wide modulation of reaction control system for reusable launch vehicle," *Missiles and Guidance*, vol. 26, no. 4, pp. 313–316, 2006 (Chinese).
- [29] W. C. Durham, "Constrained control allocation: three-moment problem," *Journal of Guidance, Control, and Dynamics*, vol. 17, no. 2, pp. 330–336, 1994.
- [30] J. A. Paradiso, "A highly adaptable method of managing jets and aerosurfaces for control of aerospace vehicles," *Journal of Guidance, Control and Dynamics*, vol. 14, no. 1, pp. 44–50, 1991.
- [31] H. Chenglong, *Research of Guidance and Control Technologies for Reusable Launch Vehicle Sub-Orbital Ascent Flight*, 2010 (Chinese).
- [32] P. Calhoun, "An entry flight controls analysis for a reusable launch vehicle," Tech. Rep. AIAA-2000-1046, 2000.
- [33] R. R. Costa, Q. P. Chu, and J. A. Mulder, "Re-entry flight controller design using nonlinear dynamic inversion," Tech. Rep. AIAA-2001-37110, 2001.
- [34] D. S. Rubenstein and D. W. Carter, "Attitude control system design for return of the Kistler KI Orbital Vehicle," *Journal of Spacecraft and Rockets*, vol. 37, no. 2, pp. 273–282, 2000.
- [35] H. Weijun and Z. Jun, "A design method of controller for reaction control system in high atmosphere," *Computer Simulation*, vol. 27, no. 3, pp. 89–93, 2010 (Chinese).
- [36] L. Wu, Y. Huang, and C. He, "Reusable launch vehicle lateral control design on suborbital reentry," in *Proceedings of the 2008 2nd International Symposium on Systems and Control in Aerospace and Astronautics (ISSCAA '08)*, Shenzhen, China, December 2008.